Journal of the Korean Physical Society, Vol. 52, February 2008, pp. S132∼S137

Microstructure Control of Fe Catalyst Films for the Growth of Multiwalled Carbon Nanotube Arrays

Guo-an CHENG,* Hua-ping LIU, Rui-ting ZHENG, Yong ZHAO and Chang-lin LIANG
Key Laboratory of Radiation Beam Technology and Material Modification of the Education Ministry, Department of Materials Science and Engineering, Institute of Low-Energy Nuclear Physics, Beijing Normal University, Beijing Radiation Center, Beijing 100875, China

Fe catalyst films were deposited on silicon substrates by using a metal vapor vacuum arc (MEVVA) ion deposition system for the growth of aligned multiwalled carbon nanotubes. The effects of deposition angle and film thickness on the morphologies of catalyst films before and after thermal treatment were investigated. The results show that the uniformities of both 5-nm and 10-nm films are enhanced as the deposition angle decreases. With increase from 5 nm to 10 nm, the surface uniformities of pristine films prepared at higher deposition angles (60° and 90°) are increased, while that of the films produced at 30° deposition angle is slightly decreased. The uniformity of Fe catalyst particle sizes after thermal treatment on the whole, clearly decreases as the thickness is increased from 5 nm to 10 nm in the case of the same deposition angle. 5-nm films deposited at 30° deposition angle show the most uniform features before and after thermal treatment and can be used for the synthesis of high-quality carbon nanotube arrays.

PACS numbers: 61.46.Km, 61.82.Fk, 82.45.Jn, 91.60.Ed
Keywords: Carbon nanotubes, Arrays, Fe catalyst film, Thickness, Deposition angle

I. INTRODUCTION

Carbon nanotubes have the potential to be used for nano-electronic devices and electron field-emission sources [1–4], due to their one-dimensional nanostructure, high curvature ratio of tip, high conductivity and thermal stability. For this purpose, it is highly desirable to controllably prepare well-aligned and highly pure carbon nanotube arrays with uniform diameters, so that the properties of individual nanotubes can be easily assessed and incorporated effectively into devices. However, the controllable synthesis of carbon nanotubes is still one of the challenges for their application. Much research is still focused on the synthesis of aligned carbon nanotubes to understand the nucleation mechanism and optimize the growth processes [5–10]. Among the different methods, the CVD method has been widely used, as it allows the controlled, selective growth of carbon nanotubes directly on a substrate, as well as bulk production [11].

It is well known that metal catalysis is the key for the formation of carbon nanotubes in the CVD process [12], and well-dispersed substrate-supported nano-scale catalyst particles can catalyze well-aligned and pure carbon nanotube arrays. Various methods have been developed to prepare nano-scale catalysts [12–15]. In many cases, the catalyst is initially deposited in the form of a thin film by magnetic sputtering or thermal evaporation, followed by high-temperature processing in gases like hydrogen, nitrogen, or ammonia, to form small nanoparticles. However, the preparation process of catalyst films has a great influence on pristine film microstructures and the corresponding distribution of catalyst particles formed during thermal treatment, and it therefore determines the morphologies of aligned carbon nanotubes.

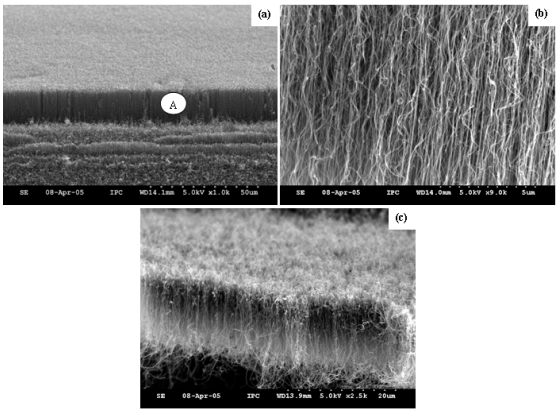

Fig. 1. FESEM images of carbon nanotube arrays synthesized on the crosssection and front surface of the same Si substrates for 90° deposition angle to the front surface: (a) on the crosssection; (b) close view of location A in (a); (c) on the front surface.

*Corresponding Author; E-mail: gacheng@bnu.edu.cn

In our work, 5-nm-thick Fe catalyst films were deposited on silicon wafers at a 90° angle by using a metal vapor vacuum arc (MEVVA) deposition technique for the growth of multi-walled carbon nanotube arrays. Carbon nanotube arrays grown on the silicon front surface are worse aligned and curved, with many carbon particles present. In contrast, carbon nanotube arrays grown on the crosssection are well aligned and pure, as shown in Fig. 1. The difference in the morphologies of carbon nanotube arrays should result from the differential microstructures of the catalyst films on the different surfaces of silicon substrates, because the deposition angles of these surfaces with respect to the ion beams are varied during the preparation of Fe films. In this Connection, we previously investigated the effect of deposition angle on the microstructure of 5-nm-thick Fe films [17] and demonstrated the hypothesis. A relevant question is whether the effect of deposition angle on the microstructure of variously thick catalyst films is the same, and also whether a uniform distribution of Fe catalyst particles can be made for variously thick catalyst films by controlling the deposition angle. For such comparison, we here systematically studied the effect of deposition angles on the microstructure of 5-nm and 10-nm catalyst films by following the same experimental procedure.

II. EXPERIMENTAL DETAILS

N-type (111) silicon wafers with resistivity of $4 - 4.8$ Ωcm and a native oxide layer were used as substrates. Fe thin films were deposited on the chemically cleaned Si substrates by a metal vapor vacuum arc (MEVVA) ion deposition system at room temperature. Figure 2 shows a schematic diagram of the apparatus. Fe plasma is generated by an arc between the cathode (Fe bar) and anode, and induced into the chamber through a magnetic plasma duct in which large particles are filtered. Fe ions are attracted by negative bias (100 V) on the silicon wafers and deposited on the surfaces. During deposition, the base pressure of the chamber is kept at 10^{-4} Pa. Before deposition, the surfaces of the silicon substrates were bombarded by Fe ions for cleaning at 3000 V negative bias to enhance the adherence of the Fe film to the Si substrates. The thickness was changed to investigate the effect of thickness on the microstructure of the Fe films.

The thermal treatment of Fe catalyst films and the synthesis of aligned carbon nanotubes were conducted in a horizontal thermal chemical vapor deposition (TCVD) system. The silicon substrates coated with different-thickness Fe nanofilms were transferred to the reaction region of the TCVD system and then heated to 600 °C in H_2, and the Fe catalyst was deoxidized for 60 min. After that, the Fe catalyst was pretreated for 10 min in NH_3 at 750 °C to form nanoparticles. For the observation of the morphological changes in the Fe films by thermal treatment, the samples were taken out at the end of the NH_3 treatment process. For the synthesis of carbon nanotubes, a gas mixture of C_2H_2 and H_2 with a ratio 90 (ml/min)/600 (ml/min) was introduced into the reaction region and the reaction proceeded for $2 \sim 30$ min. The samples were cooled in N_2 and observed by using a Field-Emission Scanning-Electron Microscope (FESEM). Atomic-Force Microscope (AFM) was used to examine the surface topologies of thepristine Fe films.

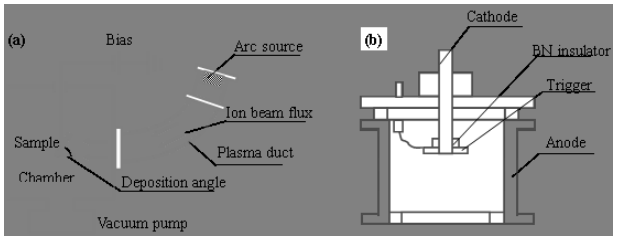

Fig. 2. (a) Schematic diagram of the metal vapor vacuum arc (MEVVA) ion deposition system; (b) arc source.

III. RESULTS AND DISCUSSION

Figure 3 shows AFM images of 5-nm and 10-nm Fe films deposited at varied angles, respectively. From Fig. 3, the surface morphologies of both films have a similar trend of change as the deposition angle decreases. Closely packed structures and large salient features on the film surfaces are observed when the incident flux arrives perpendicular to the silicon substrates. As the deposition angle decreases to 60°, the salient feature size is clearly decreased and more uniformly distributed on the substrates. As the deposition angle further decreases to 30°, columnar Fe grains with uniform size are obtained and most uniformly distributed on the substrate surface.

On comparing the 10-nm with 5-nm of Fe films, it is seen that the surface features are varied with increasing thickness of the film in the case of the same deposition angle. The valleys on the film surfaces are filled for normal incidence with an increase in thickness, and the heights of the salient features clearly decrease and hence the uniformity increases. For 60° deposition angle, the heights of the salient features do not change greatly with increasing film thickness, but spread and are more uniformly distributed on the silicon substrates. In the case of 30° incident angle, Fe nano-columns clearly grow up on increasing the thickness of the Fe film from 5 nm to 10 nm, and the heights are increased, but the uniformity slightly decreases.

For more precise analysis of the various film surface morphologies, we analyzed their surface roughness by using AFM. The experimental results are shown in Fig. 4. Figure 4 shows analysis of Mean Roughness (MR), Root-Mean-Square Roughness (RMSR), and Maximum Height (MH) on the Fe nanofilm surface with thickness of 5 nm

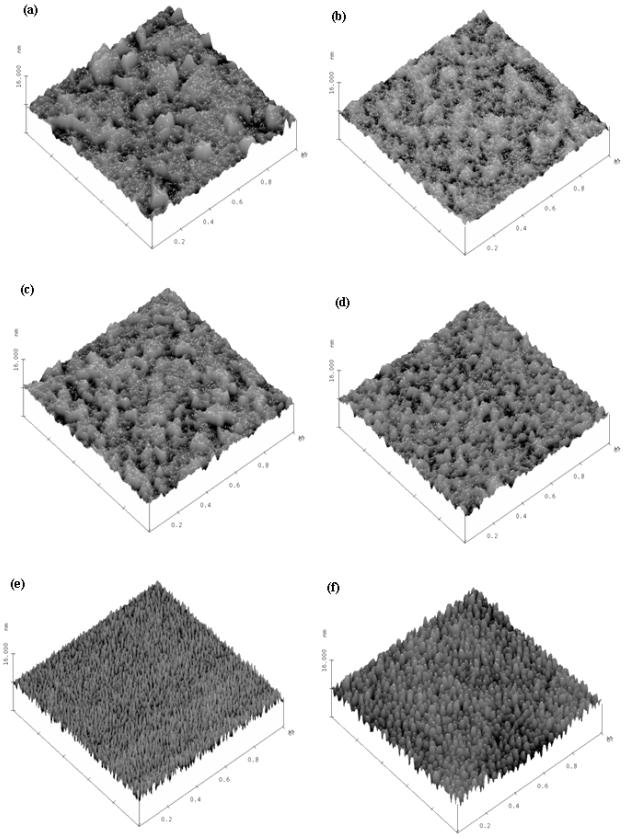

Fig. 3. AFM images of Fe deposited films for different angles. (a), (c), (e) 5 nm; (b), (d), (f) 10 nm. (a), (b) 90°; (c), (d) 60°; (e), (f) 30°.

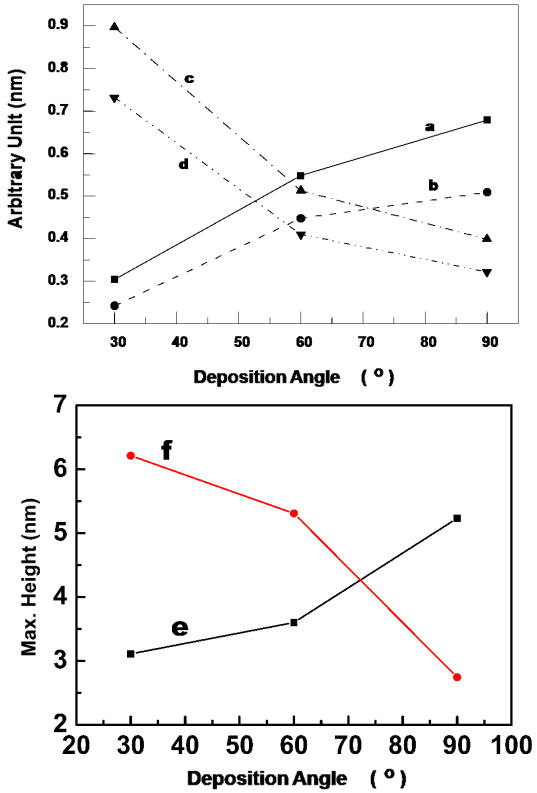

Fig. 4. Analysis of Mean Roughness (MR), Root Mean Square Roughness (RMSR), and Maximum Height (MH) on the Fe nanofilm surface with thickness of 5 nm and 10 nm, fabricated for different incident angles. a) MR for 5 nm; b) MR for 10 nm; c)RMSR for 5 nm; d) RMSR for 10 nm; e) MH for 5 nm; f) MH for 10 nm.

and 10 nm, following fabrication with different incident angles. In contrast, with a decrease of deposition angle, the roughness of 10-nm-thick Fe film increases and the roughness of 5-nm-thick Fe film decreases. With the film thickness increasing from 5 nm to 10 nm, the roughness of the film surface decreases for large incident angles but increases for small incident angle. These results well reflect the top morphologies of the films.

The above results well demonstrate that both the deposition angle and the thickness have a great influence on the microstructure of pristine catalyst iron films. Thin-film growth is a complicated process, especially for the early stage of growth [18]. The growth of thin films will start with a random distribution of nuclei which will act as seeds for further growth. If an atom arriving at a silicon substrate encounters a nucleus, it will travel along its contour and get trapped at some point [19]. With the Fe ions continuing to arrive at the substrate surface, the as-formed nuclei will grow and form islands, finally entirely covering all the substrate surface and forming a complete film. The incident iron atom arrives perpendicular to the silicon substrate surface in the case of 0° deposition angle. According to Lennard-Jones' calculation [20], an iron atom which arrives perpendicular to the film surface, will lose its excess energy in a few nanoseconds and travel only a few atomic distances during the period of accommodation. Thus, it is possible for continuously arriving iron atoms to nucleate rapidly and form small Fe crystals, which pile up to form a closely packed structure and large surface salient features. Liu *et al.* [17] also reported that closely packed structures were obtained in similar deposition conditions. With the growth of films proceeding, the atoms arriving on the top of the salient features possibly continue to travel along the slope of the salient features and fill the valleys, due to the attraction of the negative voltage applied on the substrates. Consequently, the relative height of the salient features decreases with an increase in thickness from 5 nm to 10 nm, and the film uniformity increases.

As the deposition angle is decreased to 60°, the incident atoms arrive obliquely at the film surface. Due to the conservation of parallel momentum [16,21] and the shadow mechanism [22], the nuclei will scatter more and spread more on the silicon substrate than in the case of perpendicular incidence. Fe salient features are spread and more uniformly dispersed on silicon substrates. With an increase in thickness of the films, the relative heights of the salient features are not greatly decreased, because of the shadowing effect, though some

of the atoms arriving at the top of the salient features possibly travel along the slope and fill the valleys, due to the attraction of the negative voltage on the substrates. Therefore, the roughness of films is also not changed greatly. However, the salient features are more uniformly redistributed with increasing film thickness, due to the co-effects of the shadowing effect and conservation of parallel momentum.

As the deposition angle is decreased to 30°, the arriving atoms further scatter and most uniformly nucleate on the silicon substrate because of the increasing effect of parallel momentum and shadowing [16]. With film growth proceeding, the arriving atoms cannot nucleate in the vacancies behind the as-formed nuclei in the direction given by the projection of the incident vapor beam, because of increasing shadowing effects, and they are possibly captured as soon as they arrive at the top of the as-formed nuclei. Thus, columnar nanostructures are formed and most uniformly distributed on the silicon substrate, which is clearly different from the closely packed structures of films formed in the case of the larger deposition angles (90° and 60°). We believe that the low diffusion of adatoms due to the increasing shadowing effect plays an important role in the formation of columnar Fe grains. Liu *et al.* [17] also argued that columnar structures are formed due to the low diffusion of adatoms. The roughness of the surface increases with increasing thickness, due to the increasing height of the columnar grains. At the same time, columnar Fe clusters grow up with increasing film thickness because of the increasing diffusion of Fe atoms when the vapor flux obliquely reaches the film surface at 30° deposition angle [17].

It is necessary for Fe films to be pretreated at high temperature to form nanoscale particles during the synthesis of carbon nanotubes by using the TCVD method. The distribution of Fe particles formed in the thermal treatment determines the morphologies of carbon nanotube arrays. Accordingly, we systematically investigated the distribution of Fe particles after thermal treatment of 5-nm and 10-nm films in ammonia for 10 min. The results are shown in Fig. 5. From Fig. 5, it is obvious that the distribution of Fe nanoparticles resulting from 10-nm film has a similar tendency to 5-nm-thick film with decreasing deposition angle. As the deposition angle is decreased, both the distribution range and the peaks of particle sizes decrease distinctively, and uniformity increases. However, with an increase in the thickness from 5 nm to 10 nm in case of the same deposition angle, the distribution range and peaks of particle sizes are apparently increased. The double distribution peaks of particle sizes for 10-nm-thick films are still observed even when the deposition angle is decreased to 30°, while the particle size for 5-nm film has only one narrow distribution peak (just like a Gauss distribution) ranging from several nanometers to 120 nm and centered at around 40 nm. Therefore, the uniformity of the particle size distribution decreases greatly with an increase in thickness.

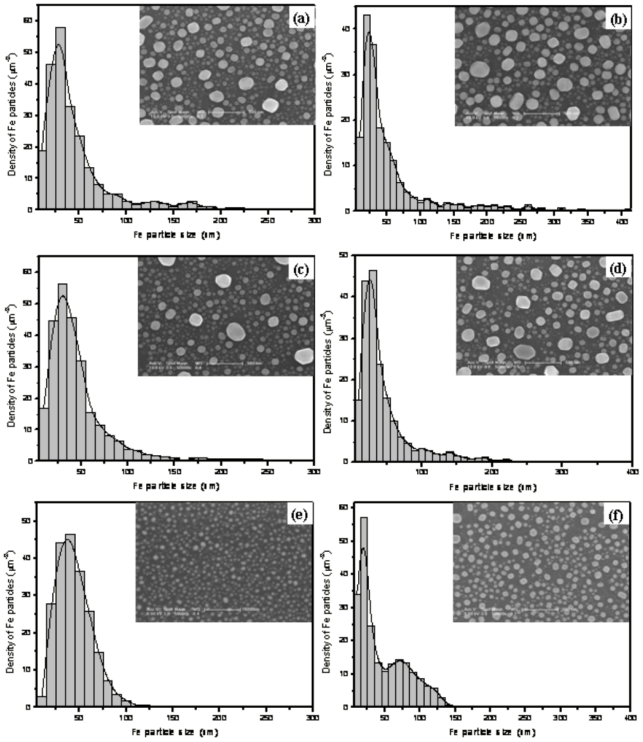

Fig. 5. Size distribution histogram of Fe particles resulting from various films after heat treatment in NH_3 for 10 min: (a), (b) 90°; (c), (d) 60°; (e), (f) 30°; (a), (c), (e) 5 nm; (b), (d), (f)10 nm. The insets show the corresponding SEM images of the distribution of nanoparticles.

From the corresponding FESEM images of the catalyst particles (the insets in Fig. 5), it is seen that the density of large particles and their size range increase clearly with increasing thickness of the film. This indicates that the results of statistical analysis are in good agreement with the distribution of Fe particles.

It is well known that there is a critical size of catalyst particles for the synthesis of carbon nanotubes in the TCVD process [23]. They are not suitable for the growth of carbon nanotubes if their size is larger than the critical size. It is found that about 90-nm catalyst particle size is the critical size in our experiment. Here, we call particles smaller than 90 nm effective particles, while particles larger than 90 nm are defined as large-size particles. It is helpful to compare the average densities and diameters of the effective particles and large-size particles resulting from 5-nm and 10-nm iron films deposited at various deposition angles, respectively (as shown in Table 1). From Table 1, it is clearly seen that both the average density and the average diameter of the large-size particles resulting from 5-nm films decrease greatly with decreasing deposition angle. When the deposition angle is decreased to 30°, the density decreases to 3.17 μm^{-2} and the corresponding average diameter decreases to 100.88 nm. Therefore, with a decrease of deposition angle, the percentage of the area of effective particles

Table 1. Statistical analysis of the large-size Fe particle (>90 nm, LSP), the effective Fe particle (0 − 90 nm, EP), and the area of effective particles (AEP) formed in thermal treatment. t stands for thickness, θ for deposition angle, δ_1 for average density, δ_2 for average diameter and A for percentage of AEP.

t	θ	δ_1 (μm^{-2})		δ_2 (nm)		A
(nm)	(°)	LSP	EP	LSP	EP	(%)
5	90	25.62	211.09	151.31	31.18	25.9
5	60	19.03	236.96	126.39	3.79	47.1
5	30	3.17	209.63	100.88	38.39	90.5
10	90	26.84	154.48	182.75	29.85	13.3
10	60	21.72	168.39	148.76	30.11	24.1
10	30	28.55	182.05	110.34	31.64	34.4

[AEP, (Average Density of effective particle) × (Square Average diameter of effective particle)] in the total catalyst area rapidly increases from 25.9% to 90.5%, and the percentage of the area of large-size particles in the total catalyst area decreases greatly. Analysis indicated that 90.5% of the area of effective particle figure in the iron catalyst was obtained at 30° deposition angle. Moreover, the effective Fe catalyst is 90.5% in the Fe catalyst with thickness of 5 nm.

From Table 1, it is seen that the percentage of the area of large-size particle figure in the total catalyst area resulting from the Fe catalyst film with thickness of 10 nm decreases much more slowly than that in the Fe catalyst film with thickness of 5 nm with a decrease of deposition angle. Especially, the average density of large-size particles for 30° deposition angle is higher than that in the case of higher deposition angles (60° and 90°), which should be ascribed to a great increase of particles in the range of 50 nm to 150 nm, as shown in Fig. 5(f). Compared to the effective particles in the Fe catalyst film with a thickness of 5 nm, both the average density and the average diameter of the effective particles resulting from the Fe catalyst film with thickness of 10 nm increase relatively slowly with a decrease of deposition angle (as shown in Table 1). A large amount of large-size particles can still be observed, even in the case of 30° deposition angle in the Fe catalyst film with a thickness of 10 nm. The percentage of the area of effective particles in the total catalyst area is only 34.4% in the Fe catalyst with thickness of 10 nm, and even less than that in the Fe catalyst with thickness of 5 nm.

The above analysis indicates that both the large salient features and an increase in the thickness of films should be responsible for the formation of large-size catalyst particles and a large range of particle sizes, and hence a decrease in the uniformity of catalyst particle distribution. The uniformity of Fe particle distribution cannot be effectively controlled, with the thickness increasing to 10 nm, by the deposition angle. Therefore, 10-nm Fe film is not suitable for the synthesis of high-quality carbon nanotube arrays. For a comparison of the catalytic

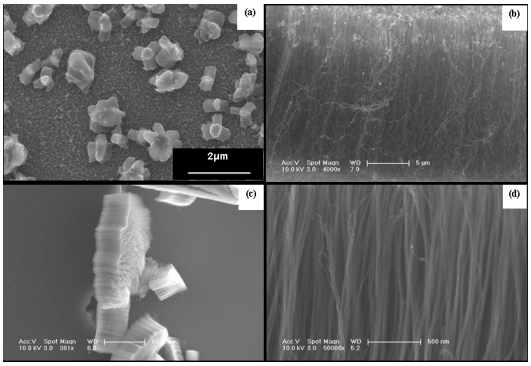

Fig. 6. FESEM images of the carbon nanotubes synthesized with 5-nm and 10-nm Fe films deposited at 30° deposition angle, respectively. (a), (b) 10 nm; (c), (d) 5 nm; (a) 2 min; (b), (c), (d) 30 min.

properties of 5-nm and 10-nm films, the relatively uniform films deposited at 30° deposition angle were used to synthesize carbon nanotube arrays. The results are shown in Fig. 6. From Fig. 6(a), it is seen that the large-size particles resulting from 10-nm films are easily covered by pyrolytic carbon and form carbon particles at the early growth stage of the carbon nanotubes. According to the growth mechanism of CNT arrays, the presence of a large number of large size Fe particles inevitably decreases the density of the nucleation of carbon nanotubes, resulting in worse alignment of carbon nanotube arrays, as shown in Fig. 6(b). In contrast, the carbon nanotube arrays synthesized with 5-nm films are well aligned and pure, and the diameters are uniform [Figs. 6(c) and (d)]. Almost all the catalyst particles participate in the growth of carbon nanotubes, because few carbon particles can be seen in the arrays and on the substrate. In our experiment, the most uniform and effective catalyst particles are also obtained from 2-nm films deposited at 30° deposition angle, but the density is lower than that in the case of 5-nm films, and hence the carbon nanotube arrays are slightly worse aligned, due to a decrease in the nucleation density of carbon nanotubes. These results well demonstrate that 5-nm Fe films deposited at 30° deposition angle are most suitable for the growth of high-quality carbon nanotube arrays.

IV. CONCLUSIONS

The morphologies and microstructures of thin Fe films can be controlled by deposition angle and film thickness, and hence the distribution of the corresponding particles formed during thermal treatment. The surface uniformity of both 5-nm and 10-nm films is enhanced with decreasing deposition angle from 90° to 30°. The Fe films deposited at 30° angle consist of columnar grains and show uniform surface features, and the corresponding particles have a narrower size distribution. With

an increase in thickness from 5 nm to 10 nm, the uniformity of pristine films is increased for higher incident angles (90° and 60°), while the result is the opposite to the case of 30° incident angle. After thermal treatment, particle-size distribution ranges have been widened with an increase in thickness and uniformity decreases. 5-nm films produced at 30° incident angle show uniform surface features, and the corresponding Fe particles with uniform size and high density are well dispersed on silicon substrate, and can therefore be used for the synthesis of well-aligned and pure multiwalled carbon nanotube arrays. However, well-distributed catalyst particles cannot be obtained by controlling the deposition angle of 10 nm-thick films, and hence they are not suitable for the growth of high-quality carbon nanotubes.

ACKNOWLEDGMENTS

This work was supported by the National Natural Science Foundation of China (NSFC, Grant No. 10575011).

REFERENCES

[1] P. G. Collins and A. Zettl, Appl. Phys. Lett. **69**, 1969 (1996).
[2] Q. H. Wang, T. D. Corrigan, J. Y. Dai, R. P. H. Chang and A. R. Krauss, Appl. Phys. Lett. **70**, 3308 (1997).
[3] S. S. Fan, M. G. Chapline, N. R. Franklin, T. W. Tombler, A. M. Cassell and H. J. Dai, Science **283**, 512(1999).
[4] S.-J. Kyung, M. Voronko, J.-H. Lee and G.-Y. Yeom, J. Korean Phys. Soc. **47**, 818 (2005).
[5] H. Huang, H. Kajiura and A. Yamada, Chem. Phys. Lett. **356**, 567 (2002).
[6] A. Thess, R. Lee, P. Nikolaev, H. Dai, P. Petit, J. Robert, C. Xu, Y. H. Lee, S. G. Kim, A. G. Rinzler, D. T. Colbert, G. E. Scuseria, D. Tománek, J. E. Fischer and R. E. Smalley, Science **273**, 483 (1996).
[7] C. Bower, O. Zhou, W. Zhu, D. J. Werder and S. Jin, Appl. Phys. Lett. **77**, 2767 (2000).
[8] H. Liu, G. Cheng, R. Zheng, Y. Zhao and C. Liang, J. Mol. Catal. A: Chem. **247**, 52 (2006).
[9] D. Takagi, Y. Homma, H. Hibino, S. Suzuki and Y. Kobayashi, Nano Lett. **6**, 2642 (2006).
[10] S. Hofmann, R. Sharma, C. Ducati, G. Du, C. Mattevi, C. Cepek, M. Cantoro, S. Pisana, A. Parvez, F. Cervantes-Sodi, A. C. Ferrari, R. Dunin-Borkowski, S. Lizzit, L. Petaccia, A. Goldoni and J. Robertson, Nano Lett. **7**, 602 (2007).
[11] K. Hata, D. N. Futaba, K. Mizuno, T. Namai, M. Yumura and S. Ijima, Science **306**, 1362 (2007).
[12] J. H. Choi, T. Y. Lee, S. H. Choi, J. H. Han, J. B. Yoo, C. Y. Park, T. W. Jung, S. G. Yu, W. K. Yi, I. T. Han and J. M. Kim, Thin Solid Films **435**, 318 (2003).
[13] H. Wang, J. Lin, C. H. A. Huan, P. Dong, J. He, S. H. Tang, W. K. Eng and T. L. J. Thong, Appl. Surf. Sci. **181**, 248 (2001).
[14] X. Y. Zhang, L. D. Zhang, G. H. Li and L. X. Zhao, Mater. Sci. Eng. A **30**, 89 (2001).
[15] M. Jung, K. Y. Eun, J. K. Lee, Y. J. Baik, K. R. Lee and J. W. Park, Diam. Rel. Mater. **10**, 1235 (2001).
[16] H. Liu, G. Cheng, Y. Zhao, R. Zheng, C. Liang, F. Zhao and T. Zhang, Surf. Coat. Technol. **201**, 938 (2006).
[17] F. Liu, M. T. Umlor, L. Shen, J. Weston, W. Eads, J. A. Barnard and G. J. Mankey, J. Appl. Phys. **85**, 5486 (1999).
[18] D. M. Wang and Z. Q. Wu, Chin. Phys. **10**, 46 (2001).
[19] L. Abelmann and C. Lodder, Thin Solid Films **305**, 1 (1997).
[20] J. E. Lennard-Jones, Proceedings of the Physical Society **49E**, 140 (1937).
[21] K. Hara, J. Sci. Hiroshima Univ. Ser. A-II **34**, 139 (1970).
[22] D. Vick, L. J. Friendrich, S. K. Dew, M. J. Brett, K. Robbie, M. Seto and T. Smy, Thin Solid Films **339**, 88 (1999).
[23] Y. T. Jang, J. H. Ahn, Y. H. Lee and B. K. Ju, Chem. Phys. Lett. **372**, 745 (2003).